LEVEL SET BASED BIMODAL SEGMENTATION WITH STATIONARY GLOBAL MINIMUM

By

Suk-Ho Lee

and

Jin Keun Seo

IMA Preprint Series # 2098

(February 2006)

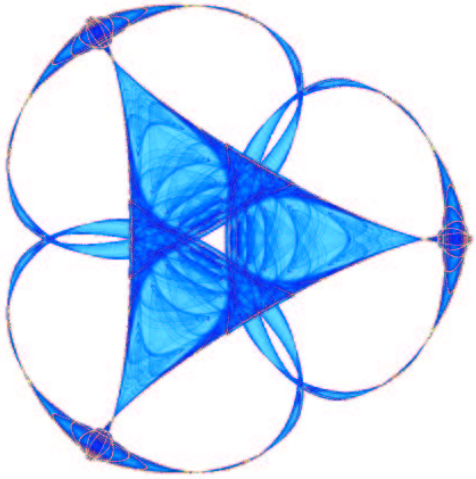

INSTITUTE FOR MATHEMATICS AND ITS APPLICATIONS

UNIVERSITY OF MINNESOTA

400 Lind Hall

207 Church Street S.E.

Minneapolis, Minnesota 55455–0436

Phone: 612/624-6066 Fax: 612/626-7370

URL: http://www.ima.umn.edu

Level Set based Bimodal Segmentation with Stationary Global Minimum

Suk-Ho Lee* and Jin Keun Seo

Yonsei University

Dept. of Math

134 Shinchon, Seodaemun-Ku, Seoul, Korea

(Tel) (822) 2123-2598, (Fax) (822) 392-6634, (Email) petrasuk@hanmail.net

Abstract:

In this paper, we propose a new level set based PDE(partial differential equation) for the purpose of bimodal segmentation. The PDE is derived from an energy functional which is a modified version of the fitting term of the Chan-Vese model [1]. The energy functional is designed to obtain a stationary global minimum, i.e., the level set function which evolves by the Euler-Lagrange equation of the energy functional has a unique convergence state. The existence of a global minimum makes the algorithm invariant to the initialization of the level set function, whereas the existence of a convergence state makes it possible to set a termination criterion on the algorithm. Furthermore, since the level set function converges to one of the two fixed values which are determined by the amount of the shifting of the Heaviside functions, an initialization of the level set function close to those values can result in a fast convergence.

KeyWords : image segmentation, Mumford-Shah model, level set, active contour, nonlinear partial differential equation.

I. Introduction

In [1], Chan and Vese have proposed a model that implements the Mumford-Shah functional [7] via the level set function for the purpose of bimodal segmentation. The segmentation is performed by an active contour model which uses the information inside regions rather than the gradients on the boundaries. The segmented regions are represented via a level set function ϕ which minimizes the following energy functional:

$$\begin{aligned} F(\phi) &= \int |\nabla H(\phi(\mathbf{r}))| d\mathbf{r} + \lambda_1 \int H(\phi(\mathbf{r}))|u_0(\mathbf{r}) - ave_{\{\phi \geq 0\}}|^2 d\mathbf{r} \\ &\quad + \lambda_2 \int H(-\phi(\mathbf{r}))|u_0(\mathbf{r}) - ave_{\{\phi < 0\}}|^2 d\mathbf{r} \end{aligned} \tag{1}$$

where λ_1, λ_2 are non-negative parameters, $u_0(\mathbf{r})$ is the given image, ϕ is the level set function, and $ave_{\{\phi \geq 0\}}, ave_{\{\phi < 0\}}$ are the average values of $u_0(\mathbf{r})$ in the 2-D regions $\{\phi < 0\}$ and $\{\phi > 0\}$,

respectively. Here, $H(\phi)$ is the one-dimensional Heaviside function with $H(s) = 1$ if $s \geq 0$, and $H(s) = 0$ if $s < 0$. To compute a minimizer ϕ for the minimization problem (1), the following parabolic equation is solved to the steady state:

$$\frac{\partial \phi}{\partial t} = |H'(\phi)| \left[\nabla \cdot \left(\frac{\nabla \phi}{|\nabla \phi|} \right) - \lambda_1 (u_0(\mathbf{r}) - ave_{\{\phi \geq 0\}})^2 + \lambda_2 (u_0(\mathbf{r}) - ave_{\{\phi < 0\}})^2 \right] \qquad (2)$$

with an appropriate initial level set function. After ϕ comes to a steady state, the zero level set of ϕ becomes the contour that separates the object from the background.

However, the minimizer of the energy sometimes becomes a local minimizer. For example, the inside region of an object cannot be detected, if the initial contour is initialized to enclose the object. This fact can also be observed from the energy functional in (1). Due to the Heaviside function in the energy functional, a change in the value of $\phi(\mathbf{r})$ has an effect on the energy only if $\phi(\mathbf{r})$ changes its sign. In other words, the ϕ function is moved in the steepest descent direction by (2), as long as there is a sign change in the value of $\phi(\mathbf{r})$ at least at one point in the next time step. However, when the zero level set settles on the outer boundary of the object, there is no sign change in ϕ in the next time step, and the algorithm stops running, leaving the inside regions non-detected. This is due to the fact that there is no decrease in the energy in the next time step.

For this reason, Chan and Vese choose a non-compactly supported smooth strictly monotone approximation of the Heaviside function, so that inside regions can be detected. However, with the approximation of the Heaviside function, the energy functional has no minimizer ϕ at all. Even after the zero level contour stops moving, the value of $\phi(\mathbf{r})$ (on both sides of the zero level contour) keeps moving to ∞ or $-\infty$. Due to the continual increase in the magnitude of the value of $\phi(\mathbf{r})$, it becomes difficult to set a termination criterion on the algorithm.

In [2] and [3], the ϕ function is restricted to $0 \leq \phi \leq 1$ to obtain a stationary solution of a model closely related to (1). In [4], $|H'(\phi)| = \delta_\epsilon(\phi)$ is replaced by 1 to obtain a fast segmentation and the ϕ function is restricted to $-1 \leq \phi \leq 1$, by quantizing the ϕ function to 1 or -1 every time step. However, it is still not guaranteed that after the quantizing step the solution remains stationary. This model is close to the model we propose in this paper, but with the proposed model, the stationary global minimum of the "fitting term" in (1) is automatically reached without a quantization step. We also prove mathematically that the proposed model computes in practice the stationary global minimum. The proposed model uses two shifted Heaviside functions. The use of the shifted Heaviside functions has two effects: First, the shifted Heaviside functions automatically choose which energy term has to be minimized depending on the current $\phi(\mathbf{r})$ value, controlling the evolution of the ϕ function such that it reaches the global minimum, regardless of the initialization of ϕ. Second, the shifted Heaviside functions restrict the value of

$\phi(\mathbf{r})$, so that the solution always becomes a stationary one. Due to these effects, the image is fully segmented including inside regions, and a stopping criterion can be imposed on the algorithm due to the stationary solution.

II. Proposed model

Instead of the "fitting term" $F = \lambda_1 \int H(\phi)|u_0(\mathbf{r}) - ave_{\{\phi\geq 0\}}|^2 d\mathbf{r} + \lambda_2 \int H(-\phi)|u_0(\mathbf{r}) - ave_{\{\phi<0\}}|^2 d\mathbf{r}$ in (1), we propose the following energy functional:

$$\begin{aligned} E(\phi) \quad &= +\lambda_1 \int_\Omega \left|u_0(\mathbf{r}) - ave_{\{\phi\geq 0\}}\right|^2 \phi(\mathbf{r})\ H(\alpha + \phi(\mathbf{r}))\ d\mathbf{r} \\ &\quad - \lambda_2 \int_\Omega \left|u_0(\mathbf{r}) - ave_{\{\phi<0\}}\right|^2 \phi(\mathbf{r})\ H(\alpha - \phi(\mathbf{r}))\ d\mathbf{r}, \end{aligned} \tag{3}$$

where α is an arbitrary small positive value, and Ω is the domain of the given image u_0. The minimization of this energy functional with regard to ϕ results in a ϕ function which zero level set becomes the contour that separates the object from the background. The minimization is performed over the set of continuous functions ϕ satisfying $\int_\Omega |D\phi| < M$ for a fixed number M. Here, $D\phi$ is the distributional gradient.

To compute the minimizer of (3), we proceed the following two step computation iteratively as in [1]: First, keeping ϕ fixed, compute $ave_{\{\phi>0\}}$ and $ave_{\{\phi<0\}}$. Next, keeping $ave_{\{\phi>0\}}$ and $ave_{\{\phi<0\}}$ fixed, we solve the following gradient descent flow equation with respect to ϕ:

$$\begin{aligned} \phi_t = \quad & -\lambda_1 |u_0(\mathbf{r}) - ave_{\{\phi\geq 0\}}|^2 \{H(\alpha + \phi(\mathbf{r})) + \phi H'(\alpha + \phi(\mathbf{r}))\} \\ & +\lambda_2 |u_0(\mathbf{r}) - ave_{\{\phi<0\}}|^2 \{H(\alpha - \phi(\mathbf{r})) - \phi H'(\alpha - \phi(\mathbf{r}))\}. \end{aligned} \tag{4}$$

We first give the rationale for the proposed energy functional, and then proceed on a rigorous analysis. Note the minus sign before the second term, which makes the model work different from the Chan-Vese model. By multiplying $\phi(\mathbf{r})$ in the energy functional, we get the effect that the energy reflects the change in the $\phi(\mathbf{r})$ value even in the absence of a sign change. This effect prevents from computing a local minimum. The shifted Heaviside functions confine the range of $\phi(\mathbf{r})$ within which the energy reflects the change. For example, if $\alpha = 0$, i.e., if we use non-shifted Heaviside functions, then the first term would reflect the change in all positive valued $\phi(\mathbf{r})$, and the second term the change in all negative valued $\phi(\mathbf{r})$. In this case, the minimizing of the first term would affect and decrease all the positive valued $\phi(\mathbf{r})$, so that they converge to zero, if $u_0(\mathbf{r}) \neq ave_{\{\phi\geq 0\}}$, while the minimizing of the second term make all the negative valued $\phi(\mathbf{r})$ converge to zero, if $u_0(\mathbf{r}) \neq ave_{\{\phi<0\}}$. However, $\phi(\mathbf{r})$ should converge to a value other than zero in the segmented regions, so that the zero level set can separate the regions. For this purpose, we shift the Heaviside functions with an amount of α. Now, without the second term, the minimization of the functional make every $\phi(\mathbf{r}) > -\alpha$ converge to $-\alpha$, while without

the first term, every $\phi(\mathbf{r}) < \alpha$ converges to α. With both the first and the second terms together, there exists also a region of competition $\{\mathbf{r} \mid -\alpha \leq \phi(\mathbf{r}) \leq \alpha\}$, i.e., a region in which the competition between the values $\left|u_0(\mathbf{r}) - ave_{\{\phi \geq 0\}}\right|^2$ and $\left|u_0(\mathbf{r}) - ave_{\{\phi < 0\}}\right|^2$ decides whether $\phi(\mathbf{r})$ converges to α or $-\alpha$. As will be explained later, it is this competition that results in the desired segmentation. It can be observed from the energy functional in (3) that the energy is minimized when every $\mathbf{r}$ at which $\left|u_0(\mathbf{r}) - ave_{\{\phi \geq 0\}}\right|^2 < \left|u_0(\mathbf{r}) - ave_{\{\phi < 0\}}\right|^2$ is classified in the region $\{\mathbf{r} \mid \phi(\mathbf{r}) = -\alpha\}$, and every $\mathbf{r}$ at which $\left|u_0(\mathbf{r}) - ave_{\{\phi \geq 0\}}\right|^2 > \left|u_0(\mathbf{r}) - ave_{\{\phi < 0\}}\right|^2$ is classified in the region $\{\mathbf{r} \mid \phi(\mathbf{r}) = \alpha\}$.

Now, we will explain and prove the effect of minimizing the proposed functional more rigorously for the following two regions: $D_{|\phi|>\alpha} = \{\mathbf{r} \in \Omega \ : \ |\phi(\mathbf{r})| > \alpha\}$ and $D_{|\phi|\leq\alpha} = \{\mathbf{r} \in \Omega \ : \ |\phi(\mathbf{r})| \leq \alpha\}$. For simplicity, and without loss of generalization, we let $\lambda_1 = \lambda_2 = 1$ afterward. We denote by $\Psi[\phi](\mathbf{r})$ the integrand of the energy functional:

$$\begin{aligned} \Psi[\phi](\mathbf{r}) := \quad & + \left|u_0(\mathbf{r}) - ave_{\{\phi \geq 0\}}\right|^2 \phi(\mathbf{r}) \ H(\alpha + \phi) \\ & - \left|u_0(\mathbf{r}) - ave_{\{\phi < 0\}}\right|^2 \phi(\mathbf{r}) \ H(\alpha - \phi), \end{aligned} \tag{5}$$

and observe the fact that in $\Psi[\phi](\mathbf{r})$ the values of $\left|u_0(\mathbf{r}) - ave_{\{\phi \geq 0\}}\right|^2$ and $\left|u_0(\mathbf{r}) - ave_{\{\phi < 0\}}\right|^2$ depend only on the zero level set, while the values of $\phi(\mathbf{r})H(\alpha + \phi)$ and $\phi(\mathbf{r})H(\alpha - \phi)$ are controlled by all the level sets.

Now, consider the case $\mathbf{r} \in D_{|\phi|>\alpha}$. If $\phi > \alpha$, then $\Psi[\phi](\mathbf{r}) = + \left|u_0(\mathbf{r}) - ave_{\{\phi \geq 0\}}\right|^2 \phi(\mathbf{r})$, and therefore, $\Psi[\phi](\mathbf{r})$ decreases as $\phi(\mathbf{r})$ decreases, until $\phi(\mathbf{r})$ reaches the boundary $\phi(\mathbf{r}) = \alpha$. Here, α acts as a boundary across which $\Psi[\phi](\mathbf{r})$ increases abruptly if $\phi(\mathbf{r}) = \alpha_- \rightarrow \alpha_+$. Otherwise, if $\phi < -\alpha$, then $\Psi[\phi](\mathbf{r})$ decreases as $\phi(\mathbf{r})$ increases and reaches the boundary $\phi(\mathbf{r}) = -\alpha$. Therefore, under the evolution equation (4), every $\phi(\mathbf{r})$ with magnitude value $|\phi(\mathbf{r})| > \alpha$ experiences a change such that $|\phi(\mathbf{r})|$ decreases, and is forced to reside between $-\alpha \leq \phi(\mathbf{r}) \leq \alpha$, i.e., every region $D_{|\phi|>\alpha}$ converts to $D_{|\phi|\leq\alpha}$. We will prove this fact, by stating and proving the following Lemma:

Lemma 2.1: If $\phi(\mathbf{r})$ is a minimizer for the energy functional $E(\phi)$ in (3), then $-\alpha \leq \phi \leq \alpha$ whenever $\Psi[\phi](\mathbf{r}) \neq 0$.

Before proving this Lemma, we give some remarks on the definition of a minimizer. Normally, a minimizer is defined as the limit of a minimizing sequence. But here, the limit would be a discontinuous function which is not in the admissible class, that is, the set of continuous functions in $BV(\Omega)$, where $BV(\Omega)$ is the class of bounded variation. This uncommon property requires to provide a meaningful definition of a minimizer that matches to the standard definition for practical applications.

Definition: A function $\phi \in BV(\Omega)$, the class of bounded variations, is said to be a local minimizer if ϕ is a piecewise continuous function satisfying the following two conditions:

1) *Small perturbation of ϕ itself.* For any subdomain D of Ω, $E(\phi) < E(\phi + \epsilon g \chi_D)$ for any continuously differentiable function g, and for a sufficiently small $\epsilon \in \mathbf{R}$. Here, χ_D is the characteristic function of D.
2) *Small perturbation of the boundary of the set* $\{\phi < 0\}$. If $\mathbf{r}^*$ lies in the boundary of the set $\{\phi < 0\}$, then $E(\phi) < E(\phi + g\chi_{B_\epsilon^-(\mathbf{r}_*)})$ and $E(\phi) < E(\phi + g\chi_{B_\epsilon^+(\mathbf{r}_*)})$ for any continuously differentiable function g. Here, $B_\epsilon^-(\mathbf{r}_*) = B_\epsilon(\mathbf{r}_*) \cap \{\phi < 0\}$ and $B_\epsilon^+(\mathbf{r}_*) = B_\epsilon(\mathbf{r}_*) \cap \{\phi \geq 0\}$, where $B_\epsilon(\mathbf{r}_*)$ is the disk centered at $\mathbf{r}_*$ with a radius ϵ .

This definition is somewhat based on observations that ϕ converges to piecewise continuous functions. With this definition given, the proof is provided in appendix I.

We give some remarks on the case when there exists a point $\mathbf{r}^*$ such that $\Psi[\phi](\mathbf{r}^*) = 0$ and $|\phi(\mathbf{r}^*)| > \alpha$ in the steady state. This case happens if $u_0(\mathbf{r}^*) = ave_{\{\phi>0\}}$, when $\phi(\mathbf{r}^*) > 0$, or $u_0(\mathbf{r}^*) = ave_{\{\phi<0\}}$ when $\phi(\mathbf{r}^*) < 0$. However, we can observe that even in this case the point $\mathbf{r}^*$ is rightly classified. This is due to the fact that $\phi(\mathbf{r}^*)$ has a plus sign if $u_0(\mathbf{r}^*) = ave_{\{\phi>0\}}$, and a minus sign if $u_0(\mathbf{r}^*) = ave_{\{\phi<0\}}$, which are the right signs, since we want to assign a plus sign to $\phi(\mathbf{r}^*)$ if $|u_0(\mathbf{r}^*) - ave_{\{\phi>0\}}|^2$ is smallest, and a minus sign if $|u_0(\mathbf{r}^*) - ave_{\{\phi<0\}}|^2$ is smallest. However, it is very unlikely that such a point can exist in the steady state (in our numerical experiments we have never met such a point so far). This is due to the fact that the $\Psi[\phi](\mathbf{r}^*) = 0$ state can happen only temporarily (if ever), as the ϕ function continually evolves under the equation (4). As a result, at the steady state, ϕ usually falls into the interval $-\alpha \leq \phi(\mathbf{r}) \leq \alpha$ at all points.

Now, we consider the case $\mathbf{r} \in D_{|\phi|\leq\alpha}$. In this case $H(\alpha - \phi(\mathbf{r})) = H(\alpha + \phi(\mathbf{r})) = 1$. Hence, $\Psi[\phi](\mathbf{r})$ is simplified as

$$\Psi[\phi](\mathbf{r}) = \phi(\mathbf{r})\Lambda_\phi(\mathbf{r}),$$

where we define $\Lambda_\phi(\mathbf{r}) := \left|u_0(\mathbf{r}) - ave_{\{\phi\geq 0\}}\right|^2 - \left|u_0(\mathbf{r}) - ave_{\{\phi<0\}}\right|^2$. We can easily see that the minimizer is

$$\phi(\mathbf{r}) = \begin{cases} -\alpha & \text{if } \Lambda_\phi(\mathbf{r}) > 0 \quad (\left|u_0(\mathbf{r}) - ave_{\{\phi\geq 0\}}\right|^2 > \left|u_0(\mathbf{r}) - ave_{\{\phi<0\}}\right|^2) \\ \alpha & \text{if } \Lambda_\phi(\mathbf{r}) < 0 \quad (\left|u_0(\mathbf{r}) - ave_{\{\phi\geq 0\}}\right|^2 < \left|u_0(\mathbf{r}) - ave_{\{\phi<0\}}\right|^2), \end{cases}$$

resulting in the right classification. Observing this fact, and keeping Lemma 2.1 in mind, we are now ready to state the following theorem:

Theorem 2.2: Assume u_0 is a continuous function. If $\phi(\mathbf{r})$ is a minimizer for the energy functional $E(\phi)$ in (3), then $\text{sign}(\Lambda_\phi(\mathbf{r}))\phi(\mathbf{r}) = -\alpha$, i.e., $\phi(\mathbf{r}) = -\text{sign}(\Lambda_\phi(\mathbf{r}))\alpha$, whenever

$\text{sign}(\Lambda_\phi(\mathbf{r})) \neq 0$.

Here,

$$\text{sign}(\Lambda_\phi(\mathbf{r})) := \begin{cases} 1 & \text{if } \Lambda_\phi(\mathbf{r}) > 0 \\ -1 & \text{if } \Lambda_\phi(\mathbf{r}) < 0 \\ 0 & \text{if } \Lambda_\phi(\mathbf{r}) = 0. \end{cases}$$

Before proving the theorem, we want to remark the continuity condition of the image u_0. Indeed, one may generalize theorem 2.2 for any image $u_0 \in BV(\Omega)$ that is a piecewise continuous function, but the proof would be very laborious, lengthy, and unreadable for readers. Therefore, for the sake of simplicity we state and prove the theorem only for the case that u_0 is continuous. However, note that an image can be approximated by a continuous function, e.g., by convolving it with a Gaussian Kernel, which is a blurred version of the original image, and theorem 2.2 will hold in this case. Furthermore, the original image can be viewed as the limit of the blurred version. The proof of theorem 2.2 is provided in the appendix II.

If the image is a binary image, we can prove that it can be completely segmented by the proposed model, based on theorem 2.2. Consider a binary image u_0 defined in a domain Ω in $\mathbf{R}^2$. Let $D_1, D_2, \cdots, D_N$ be subdomains of Ω such that $\overline{D_j} \cap \overline{D_i} = \emptyset$ whenever $i \neq j$. Let $D = \cup_{j=1}^{N} D_j$. We consider a binary image u_0 that is constant in D and in $\Omega \setminus \overline{D}$. The following theorem holds.

Theorem 2.3: Suppose u_0 is a binary image with $u_0 = 2$ in D and $u_0 = 1$ otherwise. Then the energy functional (3) has exactly two local minimizers. Moreover, both local minimizers have the same energy $-2\alpha(|\Omega| + |D|)$ and a minimizer ϕ satisfies one of the followings:

$$\overline{D} = \overline{\{\mathbf{r} \in \Omega \ : \ \phi(\mathbf{r}) < 0\}} \quad \text{or} \quad \overline{D} = \overline{\{\mathbf{r} \in \Omega \ : \ \phi(\mathbf{r}) \geq 0\}}.$$

This theorem can be generalized in various ways, and the proof is given in appendix III. As a conclusion of this section, and based on theorem 2.2, we can state that, in practice, the proposed model performs a complete segmentation regardless of the initialization. However, as will be explained in section IV, a proper initialization can result in a very fast and direct segmentation, which omits the evolution of the contour.

Regularizing terms such as the minimization of the length of the contour can be added via the method proposed in [4]. Another way of adding regularizing terms would be to add them after the zero level set has come to a steady state. This prevents the conflict between the minimization of the length and the detection of small inside regions.

III. Imposition of a termination criterion

It is important for a segmentation algorithm to have a stationary solution, so that a vision system that employs the algorithm can determine if the desired segmentation has been performed and the computation be terminated. Due to the everlasting increase in the magnitude of ϕ, it is difficult to impose a termination criterion on the Chan-Vese model. Obviously, a termination criterion based on the comparison between the $\phi(\mathbf{r})$ values of the current and the previous step will not work. A termination criterion based on the expiration of sign changes in the $\phi(\mathbf{r})$ values is not an appropriate choice either, since the algorithm will fail to detect certain regions, e.g., inside regions. Of course, one could set a predefined number of iterations large enough for the algorithm to detect all regions in the image domain, but then the optimal speed cannot be obtained. Furthermore, the number of iterations is dependent on the initialization of the ϕ function and the kind of image, making it difficult to predefine the number. In comparison, the stationarity of the solution of the proposed model makes it easy to set a termination criterion on the algorithm based on the measurement of the convergency of ϕ. For example, as we know that $|\phi(\mathbf{r})|$ converges to α, we can define the "normalized step difference energy"(NSDE) as follows:

$$NSDE = \frac{\| |\phi(\mathbf{r})| - \alpha| \|^2}{\|\phi(\mathbf{r})\|^2}. \tag{6}$$

Then we can just measure the NSDE every time step, and terminate the algorithm if the NSDE becomes very small. We show the graph of the NSDE of the proposed model in the experiments.

IV. Proposed initialization for fast convergence

Theorem 2.2 guarantees that the proposed model computes the global minimum regardless of the initialization, i.e., the convergence of the ϕ value to either α or $-\alpha$ is irrespective of the initial ϕ function. This means that we can start with any initial ϕ function, and obtain the same ϕ function in the steady state, that is, the same segmentation result, given that the initial ϕ function contains both positive and negative values, which is required for the initial computation of $ave_{\{\phi>0\}}$ and $ave_{\{\phi<0\}}$. If we choose the initialization of the ϕ function as a signed distance function, we obtain an active contour evolution, having the additional capability to detect inside regions.

However, since the proposed model is invariant to the initialization of ϕ, a better initialization would be one that is "close" to the true solution, to obtain a fast convergence. Since ϕ converges either to α or $-\alpha$, which can be set arbitrarily close to zero, an initialization close to the true solution would be one that is also close to zero. In our experiments, we simply initialized half of the domain with $\phi = -1$ and the other half with $\phi = 1$. With such an initialization, the image is segmented without a contour evolution, and the ϕ function converges after a few iterations.

V. EXPERIMENTAL RESULTS

We perform several experiments to show the segmentation capability of the proposed model, and to verify the computation of the stationary global minimum. We implemented the proposed scheme simply with an explicit difference scheme. The implementation of the Heaviside function $H(\cdot)$ can be done exactly using a max function, which is defined as

$$max(a,0) = \begin{cases} a & \text{if } a \geq 0 \\ 0 & \text{if } a < 0. \end{cases}$$

For the implementation of $H'(\cdot)$, we used the compactly supported regularized version in [1]. In this case, it should be taken care of that the value of $H'(\cdot)$ is not too large, and the supported region is small, otherwise this can result in oscillations around the desired steady state, if we use a small value for α in (4). In all experiments we let $\lambda_1 = \lambda_2 = 0.5$.

In Fig. 1 and Fig. 2, we show that the proposed model can detect different objects of different intensities, and compare the results obtained from two different initializations of the ϕ function. The first row of Fig. 1 shows the evolution of an active contour, with the ϕ function initialized as a signed distance function. The second row of Fig. 1 shows the corresponding evolution of the ϕ function. It can be observed that the proposed model fully segments the image. The first row of Fig. 2 shows the segmentation with a very simple initial ϕ function, having a value of -1 for the left half domain and 1 for the right half domain. With this initialization, the boundary is captured after just a few iterations without the evolution of the contour, e.g., the contour in Fig. 2(c) is the result after one iteration from that of Fig. 2(b). The number of iterations (given in the captions) is considerably small compared to that with the signed distance function initialization. Figure 2(e) and Fig. 2(j) are the converged states. It can be observed from Fig. 1 and Fig. 2 that the ϕ value has converged to 4 in the object and -4 in the background for both initializations, since we set $\alpha = 4$.

In Fig. 3, we compared the segmentation results of the proposed model and the Chan-Vese model using a compact supported Heaviside function. It can be seen that with a compact supported Heaviside function, the Chan-Vese model fails to detect the inside region and objects that are far from the zero level set, whereas with the proposed model, which also uses compact supported Heaviside functions (in fact the exact implementation of the Heaviside function), all the regions are detected.

Figure 4 shows the result on a blurred image which boundaries are not likely to be captured by a gradient based active contour. As can be seen, the proposed model segments the image well. In Fig. 5, it is shown that our model can work on a noisy image, even without a curvature term, if the noise level is not too high. If the image is very noisy, then we can incorporate the curvature

term to deal with the noise. Figure 6 shows results of performing the proposed model on some real pictures. The bimodal segmentation classifies all the pixels into two regions according to the competition between their brightness values.

Next, we show the role of the parameter α in the model. Figure 7 shows experiments on the "Baboon" image, with different values of α. The value α determines the global minimum of the energy functional in (3) according to theorem 2.2, i.e., it determines the value to which $\phi(\mathbf{r})$ converges. Thus, if we set $\alpha = 4$, every $\phi(\mathbf{r})$ converges either to 4 or to -4, whereas if we set $\alpha = 10$, they converge to 10 or -10, as can be seen from the results in Fig. 7. The segmentation results are the same, that is, $\phi(\mathbf{r})$ has the same sign regardless of the value of α, but the magnitude of $\phi(\mathbf{r})$ becomes different. With a large value of α, the true solution becomes far from zero, and thus with an initialization close to zero, it will take more time until ϕ converges than with a small value of α, as the number of iterations in Fig. 7 shows. Therefore, with the proposed initialization, it is desirable to set a small value for α to obtain a fast convergence. However, if α becomes too small, some oscillations may be introduced due to the approximation of H' and the use of a two step algorithm. We find that $\alpha > 0.5$ is large enough to avoid oscillations.

Figure 8 shows the evolutions of the ϕ functions in the Chan-Vese model and the proposed model. As can be seen, the magnitude of ϕ continues to increase with the Chan-Vese model, whereas with the proposed model, ϕ converges. As was explained in section III, the everlasting change in the magnitude of ϕ in the Chan-Vese model makes it difficult to set a termination criterion on the model. In Fig. 9, we show the NSDE, which was defined in section III, of the proposed model. We used the "Baboon" image, with $\alpha = 4$, and the proposed initialization. Here, the NSDE drops almost to zero after 9 iterations, which shows that the solution has converged. Therefore, we can impose a termination criterion on the proposed model, by stopping the algorithm, for example, if NSDE< 0.1.

VI. Conclusion

We proposed a new energy functional for the purpose of bimodal segmentation that has a stationary global minimum. The existence of a global minimum guarantees that a vision system which employs the algorithm is sure to capture the desired object instead of an undesired one. The stationarity of the solution makes it possible to set a reasonable termination criterion on the algorithm. This makes a vision system that employs the algorithm capable of automatically determining if the desired segmentation has been performed and the computation be terminated. Furthermore, since the true solution of the functional is predictable, an initialization close to the true solution can result in a very fast segmentation process, making it possible to be adopted by

real-time systems. Due to the above mentioned properties, we expect that the proposed algorithm will be useful for real-time applications, e.g., the application of motion tracking by surveillance camera systems, where motion information can be included in the segmentation process. This is the topic of our further study.

REFERENCES

[1] T.F. Chan and L.A. Vese, "Active contours without edges," IEEE Trans. on Image Processing, vol. 10, no. 2, pp.266-277, Feb. 2001.

[2] T.F. Chan, S. Esedoḡlu, and M. Nikolova, "Algorithms for Finding Global Minimizers of Image Segmentation and Denoising Models," UCLA CAM Report 04-54, 2004.

[3] X.Bresson, S. Esedoḡlu, P. Vandergheynst, J.P. Thiran, and S. Osher, "Global minimizers of the active contour /snake model," UCLA CAM Report 05-04, 2005.

[4] Gibou, F. and Fedkiw, R., "A Fast Hybrid k-Means Level Set Algorithm for Segmentation," 4th Annual Hawaii International Conference on Statistics and Mathematics, pp. 281-291, 2005. Stanford Technical Report, November 2002.

[5] B. Appleton and H. Talbot, "Globally Optimal Geodesic Active Contours," Journal of Mathematical Imaging and Vision, vol. 23, no. 1, pp. 67-86, 2005.

[6] Rousson, M. Deriche, R., "A variational framework for active and adaptative segmentation of vector valued images Motion and Video Computing," Proc. IEEE Workshop Motion and Video Computing, pp. 56-61, Dec. 2002.

[7] D. Mumford and J. Shah, "Optimal approximation by piecewise smooth functions and associated variational problems," Commun. Pure Appl. Math, vol. 42, pp. 577-685, 1989.

[8] G. Aubert and L. Vese, "A variational method in image recovery," SIAM J. Numer. Anal., vol. 34, no. 5, pp. 1948-1979, 1997.

[9] H.-K. Zhao, T. Chan, B. Merriman, and S. Osher, "A variational level set approach to multiphase motion," J. Comput. Phys., vol. 127, pp. 179-195, 1996.

[10] G.J. McLachlan, D. Peel, *Finite Mixture Models*. Wiley Series in probability and statistics, vol. 84 of statistics, Dekker, 2000.

APPENDIX I
PROOF OF LEMMA 2.1.

Suppose there exist $\mathbf{r}_0$ such that $|\phi(\mathbf{r}_0)| > \alpha$ and ϕ is continuous at $\mathbf{r}_0$. Observe that

$$\Psi[\phi](\mathbf{r}) := \begin{cases} \left|u_0(\mathbf{r}) - ave_{\{\phi\geq 0\}}\right|^2 \phi(\mathbf{r}) & \text{if } \phi(\mathbf{r}) > \alpha \\ -\left|u_0(\mathbf{r}) - ave_{\{\phi< 0\}}\right|^2 \phi(\mathbf{r}) & \text{if } \phi(\mathbf{r}) < -\alpha \end{cases}$$

We can choose $\epsilon > 0$ such that $\phi(\mathbf{r}) > \alpha$ (or $\phi(\mathbf{r}) < -\alpha$) for $B_\epsilon(\mathbf{r}_0)$, the disk centered at $\mathbf{r}_0$ with the radius ϵ. Now, define the infinitesimal variation in ϕ as

$$\eta_\phi(\mathbf{r}) = -\epsilon \frac{\phi(\mathbf{r})}{|\phi(\mathbf{r})|} \; [|\phi(\mathbf{r})| - \alpha] \, \chi_{B_\epsilon(\mathbf{r}_0)}(\mathbf{r}),$$

where χ_B is the characteristic function of B. With this variation in ϕ, the averages do not change: $ave_{\{\phi<0\}} = ave_{\{\phi+\eta_\phi<0\}}$ and $ave_{\{\phi\geq 0\}} = ave_{\{\phi+\eta_\phi\geq 0\}}$. Hence,

$$\Psi[\phi + \eta_\phi](\mathbf{r}) = \Psi[\phi](\mathbf{r}) \quad \text{ for } \mathbf{r} \notin B_\epsilon(\mathbf{r}_0).$$

Now, consider the case that $\mathbf{r} \in B_\epsilon(\mathbf{r}_0)$. If $\phi(\mathbf{r}_0) > \alpha$ and $\mathbf{r} \in B_\epsilon(\mathbf{r}_0)$, we have

$$\begin{aligned}\Psi[\phi+\eta_\phi](\mathbf{r}) - \Psi[\phi](\mathbf{r}) &= -\epsilon \left|u_0(\mathbf{r}) - ave_{\{\phi\geq 0\}}\right|^2 \frac{\phi(\mathbf{r})}{|\phi(\mathbf{r})|}\ [|\phi(\mathbf{r})| - \alpha] \\ &= -\epsilon \left|u_0(\mathbf{r}) - ave_{\{\phi\geq 0\}}\right|^2\ [|\phi(\mathbf{r})| - \alpha] \leq 0,\end{aligned}$$

where the equality holds only if $u(\mathbf{r}) = ave_{\{\phi\geq 0\}}$, or $|\phi(\mathbf{r})| = \alpha$. Note that $u_0(\mathbf{r}) = ave_{\{\phi\geq 0\}}$ implies $\Psi[\phi](\mathbf{r}) = 0$, since $\Psi[\phi](\mathbf{r}) = \left|u_0(\mathbf{r}) - ave_{\{\phi\geq 0\}}\right|^2 \phi(\mathbf{r})$.
Similarly, if $\phi(\mathbf{r}_0) < -\alpha$ and $\mathbf{r} \in B_\epsilon(\mathbf{r}_0)$, we have

$$\begin{aligned}\Psi[\phi+\eta_\phi](\mathbf{r}) - \Psi[\phi](\mathbf{r}) &= \epsilon \left|u_0(\mathbf{r}) - ave_{\{\phi<0\}}\right|^2 \frac{\phi(\mathbf{r})}{|\phi(\mathbf{r})|}\ [|\phi(\mathbf{r})| - \alpha] \\ &= -\epsilon \left|u_0(\mathbf{r}) - ave_{\{\phi<0\}}\right|^2\ [|\phi(\mathbf{r})| - \alpha] \leq 0.\end{aligned}$$

Hence, a minimizer ϕ must be $-\alpha\ \leq \phi(\mathbf{r})\ \leq\ \alpha$, whenever $\Psi[\phi](\mathbf{r}) \neq 0$. This completes the proof. □

APPENDIX II
PROOF OF THEOREM 2.2.

By Lemma 2.1, we have $-\alpha \leq \phi \leq \alpha$, whenever $\Lambda_\phi(\mathbf{r}) \neq 0$. It remains to consider the case where $-\alpha \leq \phi \leq \alpha$. We define the infinitesimal variation in ϕ as

$$\eta_\phi(\mathbf{r}) = -\frac{\epsilon}{2\alpha}|\phi(\mathbf{r})|\left[\phi(\mathbf{r}) + \alpha\ \text{sign}(\Lambda_\phi(\mathbf{r}))\right],$$

where $0 < \epsilon < 1$. With this variation of ϕ, $\{\phi + \eta_\phi < 0\} = \{\phi < 0\}$, so $\Lambda_\phi(\mathbf{r}) = \Lambda_{\phi+\eta_\phi}(\mathbf{r})$. Hence,

$$\begin{aligned}\Psi[\phi+\eta_\phi](\mathbf{r}) - \Psi[\phi](\mathbf{r}) &= -\tfrac{\epsilon}{2\alpha}|\phi(\mathbf{r})|\left[\phi(\mathbf{r}) + \alpha\ \text{sign}(\Lambda_\phi(\mathbf{r}))\right]\Lambda_\phi(\mathbf{r}) \\ &= -\tfrac{\epsilon}{2\alpha}|\phi(\mathbf{r})|\left[\ \phi(\mathbf{r})\Lambda_\phi(\mathbf{r}) + \alpha\ |\Lambda_\phi(\mathbf{r})|\ \right]\end{aligned}$$

From the assumption that $|\phi| < \alpha$, we have

$$\Psi[\phi+\eta_\phi](\mathbf{r}) \leq \Psi[\phi](\mathbf{r}).$$

The equality holds only when $\text{sign}(\Lambda_\phi(\mathbf{r}))\phi(\mathbf{r}) = 0, -\alpha$. This means that if $\phi(\mathbf{r})$ is to be a minimizer, then $\phi(\mathbf{r}) = 0$ or $\phi(\mathbf{r}) = -\text{sign}(\Lambda_\phi(\mathbf{r}))\alpha$.

It remains to prove that $\phi(\mathbf{r}) = 0$ implies $\text{sign}(\Lambda_\phi(\mathbf{r})) = 0$. Since we have shown that $\phi(\mathbf{r}) \in \{-\alpha, 0,\ \alpha\}$, and keeping in mind the definition of ϕ being a piecewise continuous function, it suffices to prove that the set $U := \{\mathbf{r}\ :\ \phi(\mathbf{r}) = 0 \text{ and } \text{sign}(\Lambda_\phi(\mathbf{r})) \neq 0\}$ does not contain any interior point.

To derive a contradiction, suppose U has an interior point $\mathbf{r}_*$. Then, there exists a small $\epsilon > 0$ so that $B_\epsilon(\mathbf{r}_*)$, the disk centered at $\mathbf{r}_*$ and having a radius ϵ, is contained in U. This time, we define the infinitesimal variation in ϕ as

$$\eta_\phi(\mathbf{r}) = -\epsilon\ \chi_{B_\epsilon(\mathbf{r}_*)}(\mathbf{r})\ \text{sign}(\Lambda_\phi(\mathbf{r})).$$

Then, for $\mathbf{r} \in B_\epsilon(\mathbf{r}_*)$, we have

$$\begin{aligned}\Psi[\phi+\eta_\phi](\mathbf{r}) - \Psi[\phi](\mathbf{r}) &= (\phi(\mathbf{r})+\eta_\phi(\mathbf{r}))\Lambda_{\phi+\eta_\phi}(\mathbf{r}) - \phi\Lambda_\phi(\mathbf{r}) \\ &= -\epsilon \ \text{sign}(\Lambda_\phi(\mathbf{r}))\ \Lambda_{\phi+\eta_\phi}(\mathbf{r}) \\ &\le -\epsilon|\Lambda_\phi(\mathbf{r})| + \epsilon\left|\Lambda_{\phi+\eta_\phi}(\mathbf{r}) - \Lambda_\phi(\mathbf{r})\right|.\end{aligned}$$

Since u_0 is continuous and $\text{sign}(\Lambda_\phi(\mathbf{r})) \neq 0$ in $B_\epsilon(\mathbf{r}_*)$, $\text{sign}(\Lambda_\phi(\mathbf{r})) = \text{sign}(\Lambda_\phi(\mathbf{r}_*))$ for $\mathbf{r} \in B_\epsilon(\mathbf{r}_*)$. In the case that $\text{sign}(\Lambda_\phi(\mathbf{r}_*)) = -1$, we have $\Lambda_{\phi+\eta_\phi} = \Lambda_\phi$, and therefore

$$\Psi[\phi+\eta_\phi](\mathbf{r}) - \Psi[\phi](\mathbf{r}) = -\epsilon|\Lambda_\phi(\mathbf{r})| < 0 \quad \text{in } B_\epsilon(\mathbf{r}_*),$$

which means that ϕ is not a minimizer, a contradiction.

Next, we consider the case that $\text{sign}(\Lambda_\phi(\mathbf{r}_*)) = 1$ in $B_\epsilon(\mathbf{r}_*)$. It is easy to see that $|ave_{\{\phi+\eta_\phi\ge 0\}} - ave_{\{\phi\ge 0\}}| = O(\epsilon^2)$ and $|ave_{\{\phi+\eta_\phi<0\}} - ave_{\{\phi<0\}}| = O(\epsilon^2)$ for a small ϵ. Hence, $\left|\Lambda_{\phi+\eta_\phi}(\mathbf{r}) - \Lambda_\phi(\mathbf{r})\right| = O(\epsilon^2)$. Therefore, we can choose ϵ small enough that

$$\Lambda_\phi(\mathbf{r}) > \frac{1}{2}\Lambda_\phi(\mathbf{r}_*) \ \text{ and } \ \left|\Lambda_{\phi+\eta_\phi}(\mathbf{r}) - \Lambda_\phi(\mathbf{r})\right| \le \frac{1}{4}\Lambda_\phi(\mathbf{r}_*) \quad \text{ for } \mathbf{r} \in B_\epsilon(\mathbf{r}_*).$$

Then, for $\mathbf{r} \in B_\epsilon(\mathbf{r}_*)$, we have

$$\begin{aligned}\Psi[\phi+\eta_\phi](\mathbf{r}) - \Psi[\phi](\mathbf{r}) &= -\epsilon \ \text{sign}(\Lambda_\phi(\mathbf{r}))\ \Lambda_{\phi+\eta_\phi}(\mathbf{r}) \\ &\le -\epsilon|\Lambda_\phi(\mathbf{r})| + \epsilon\left|\Lambda_{\phi+\eta_\phi}(\mathbf{r}) - \Lambda_\phi(\mathbf{r})\right| \\ &\le -\tfrac{\epsilon}{4}\Lambda_\phi(\mathbf{r}_*) < 0,\end{aligned}$$

a contradiction. All these show that U does not contain any interior point. This means that $\phi(\mathbf{r}) = -\text{sign}(\Lambda_\phi(\mathbf{r}))\alpha$, whenever $\text{sign}(\Lambda_\phi(\mathbf{r})) \neq 0$. This completes the proof. □

APPENDIX III
PROOF OF THEOREM 2.3.

Suppose ϕ is a minimizer. Then $-\alpha \le \phi \le \alpha$ based on Lemma 2.1. For simplicity, we denote $\gamma_\phi^+ = \text{ave}_{\{\phi\ge 0\}}$ and $\gamma_\phi^- = \text{ave}_{\{\phi<0\}}$. Since $\Lambda_\phi(\mathbf{r}) = 2(\gamma_\phi^- - \gamma_\phi^+)\left(u_0 - \frac{\gamma_\phi^- + \gamma_\phi^+}{2}\right)$, we have

$$E(\phi) = 2(\gamma_\phi^- - \gamma_\phi^+)\left[\int_D \phi\left(2 - \frac{\gamma_\phi^- + \gamma_\phi^+}{2}\right)d\mathbf{r} - \int_{\Omega\setminus\bar{D}} \phi\left(\frac{\gamma_\phi^- + \gamma_\phi^+}{2} - 1\right)d\mathbf{r}\right].$$

Furthermore, since $1 < \frac{\gamma_\phi^- + \gamma_\phi^+}{2} < 2$, we have $\Lambda_\phi(\mathbf{r}) \neq 0$ provided that $\gamma_\phi^- \neq \gamma_\phi^+$.

If $\gamma_\phi^- > \gamma_\phi^+$, then it follows from Theorem 2.2 that

$$\phi(\mathbf{r}) = -\alpha \ \text{sign}(\Lambda_\phi(\mathbf{r})) = \begin{cases} -\alpha & \text{if } \mathbf{r} \in D \\ \alpha & \text{if } \mathbf{r} \in \Omega \setminus \bar{D} \end{cases}$$

In this case, $\gamma_\phi^- = 2$ and $\gamma_\phi^+ = 1$, and so

$$\Phi[\phi](\mathbf{r}) = \begin{cases} -4\alpha & \text{if } \mathbf{r} \in D \\ -2\alpha & \text{if } \mathbf{r} \in \Omega \setminus \bar{D} \end{cases} \qquad \text{and} \qquad E(\phi) = -2\alpha(|\Omega| + |D|).$$

Similarly, if $\gamma_\phi^- < \gamma_\phi^+$, we have

$$\phi(\mathbf{r}) = -\alpha \text{ sign}(\Lambda_\phi(\mathbf{r})) = \begin{cases} \alpha & \text{if } \mathbf{r} \in D \\ -\alpha & \text{if } \mathbf{r} \in \Omega \setminus \bar{D} \end{cases} \quad \text{and} \quad E(\phi) = -2\alpha(|\Omega| + |D|).$$

The above two cases provide for the fact that the two minimizers have the same energy $-\alpha|\Omega|$. It remains to show that $\gamma_\phi^+ \neq \gamma_\phi^-$. To derive a contradiction, assume that $\gamma_\phi^+ = \gamma_\phi^-$. For the following analysis, we write $E(\phi)$ as $E(\phi) = 2(\gamma_\phi^- - \gamma_\phi^+)A[\phi]$, where

$$A[\phi] := \left[\int_D \phi \left(2 - \gamma_\phi^-\right) d\mathbf{r} - \int_{\Omega \setminus \bar{D}} \phi \left(\gamma_\phi^- - 1\right) d\mathbf{r} \right].$$

Note that if $\gamma_\phi^+ = \gamma_\phi^-$, then γ_ϕ^- has to lie in the interval $1 < \gamma_\phi^- < 2$. For γ_ϕ^- to lie in this interval, at least one of the following conditions must be satisfied:

1) There exist $\mathbf{r}_* \in \partial\{\phi < 0\} \cap D$ such that $B_{\epsilon_1}(\mathbf{r}_*) \subset D$ for some $\epsilon_1 > 0$.
2) There exist $\mathbf{r}_* \in \partial\{\phi < 0\} \cap \Omega \setminus \bar{D}$ such that $B_{\epsilon_1}(\mathbf{r}_*) \subset \Omega \setminus \bar{D}$ for some $\epsilon_1 > 0$.

We will derive a contradiction only for the first condition. A contradiction for the second condition can be derived in a similar way. For the case that $A[\phi] < 0$, we choose $\eta_\phi^1 := [-\phi - \epsilon]\chi_{B_\epsilon^+}$ as the infinitesimal variation in ϕ, where $B_\epsilon^+ = B_\epsilon(\mathbf{r}_*) \cap \{\phi \geq 0\}$. For $0 < \epsilon < \epsilon_1$, we then have

$$\gamma^-_{\phi+\eta^1_\phi} > \gamma^+_{\phi+\eta^1_\phi} \quad \text{and} \quad E(\phi + \eta_\phi^1) = 2(\gamma^-_{\phi+\eta^1_\phi} - \gamma^+_{\phi+\eta^1_\phi})(A[\phi] + O(\epsilon^2)).$$

Hence, $E(\phi+\eta_\phi^1) < 0$ for a sufficiently small ϵ. However, this is not possible because we assumed that ϕ is a minimizer. This is a contradiction to the assumption.

If $A[\phi] > 0$, we choose $\eta_\phi^2 := [-\phi + \epsilon]\chi_{B_\epsilon^-}$ where $B_\epsilon^- = B_\epsilon(\mathbf{r}_*) \cap \{\phi < 0\}$. Similarly, as above, we have $E(\phi + \eta_\phi^2) < 0$ for a sufficiently small ϵ, which is again a contradiction to the assumption.

Finally, if $A[\phi] = 0$, we choose

$$\eta_\phi^3 := \epsilon \, |\phi| \, \chi_{D^-} + \eta_\phi^2 \quad \text{where } D^- = \{\phi < 0\} \cap D.$$

Then $\gamma^-_{\phi+\eta^3_\phi} - \gamma^+_{\phi+\eta^3_\phi} = \gamma^-_{\phi+\eta^2_\phi} - \gamma^+_{\phi+\eta^2_\phi} < 0$ for $0 < \epsilon < \epsilon_1$ and

$$E(\phi + \eta_\phi^3) = 2(\gamma^-_{\phi+\eta^2_\phi} - \gamma^+_{\phi+\eta^2_\phi}) \left(\epsilon \int_{D^-} |\phi| \, (2 - \gamma_\phi^-) d\mathbf{r} + O(\epsilon^2) \right).$$

Hence, $E(\phi + \eta_\phi^3) < 0$ for sufficiently small ϵ, a contradiction. All these prove that $\gamma_\phi^+ \neq \gamma_\phi^-$. This completes the proof. □

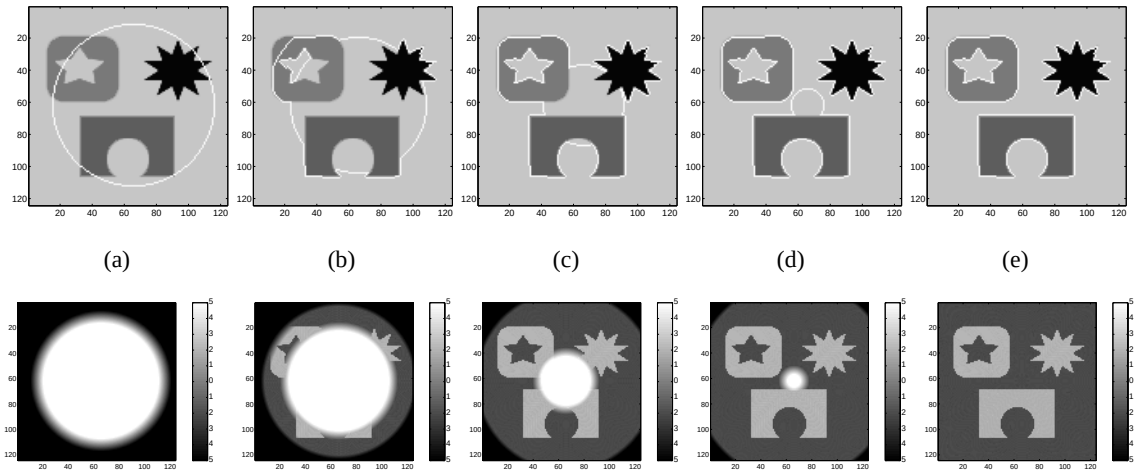

(a) (b) (c) (d) (e)

(f) (g) (h) (i) (j)

Fig. 1. Segmentation of different objects with different intensities with ϕ initialized as a signed distance function. Top row: showing the evolution of the zero level set. Bottom row: showing the evolution of the corresponding level set function. (e) and (j) are the converged results after 323 iterations.

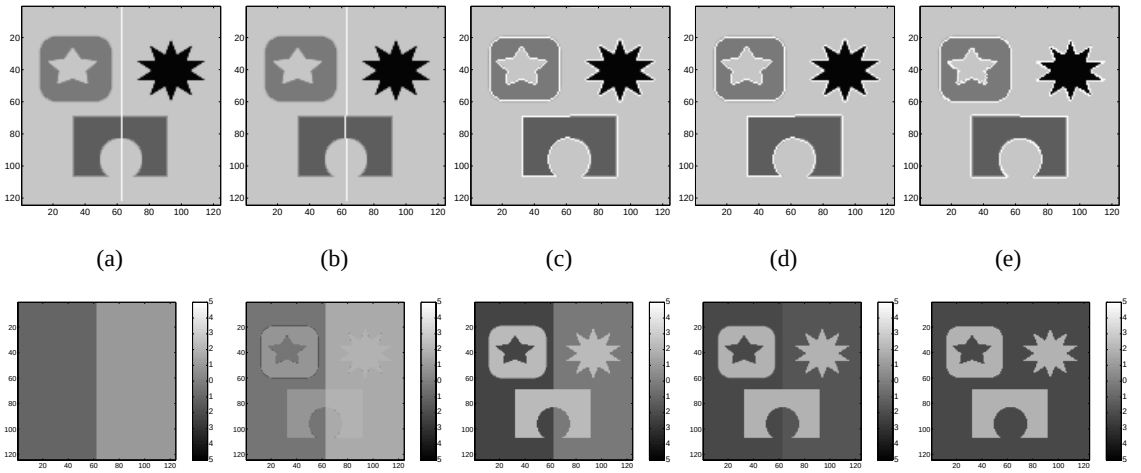

(a) (b) (c) (d) (e)

(f) (g) (h) (i) (j)

Fig. 2. Segmentation of different objects with different intensities with ϕ initialized as proposed. Top row: showing the evolution of the zero level set. Bottom row: showing the evolution of the corresponding level set function. (a),(f): initial (b),(g): after 3 iterations (c),(h): after 4 iterations (d),(i): after 6 iterations (e),(j): after 8 iterations. (e),(j) are the converged states.

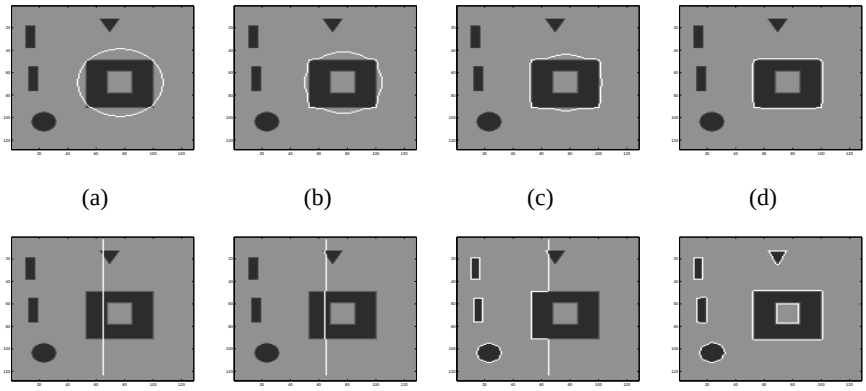

(a) (b) (c) (d)

(e) (f) (g) (h)

Fig. 3. Comparison between the segmentation results of the Chan-Vese model and the proposed model, both using compactly supported Heaviside functions. Top row: segmentation result with Chan-Vese model with compactly supported Heaviside functions. Bottom row: segmentation result with proposed model with compactly supported Heaviside functions.

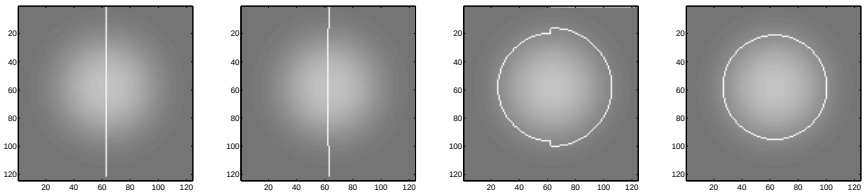

(a) (b) (c) (d)

Fig. 4. Segmentation results on a image with blurred boundaries.

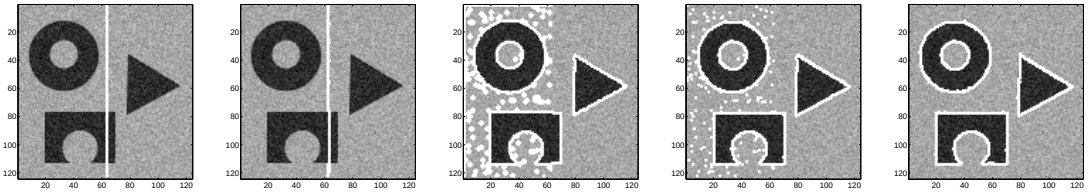

(a) (b) (c) (d) (e)

Fig. 5. Segmentation result on a noisy image where the noise level is not too high. The noise level is SNR=20dB.

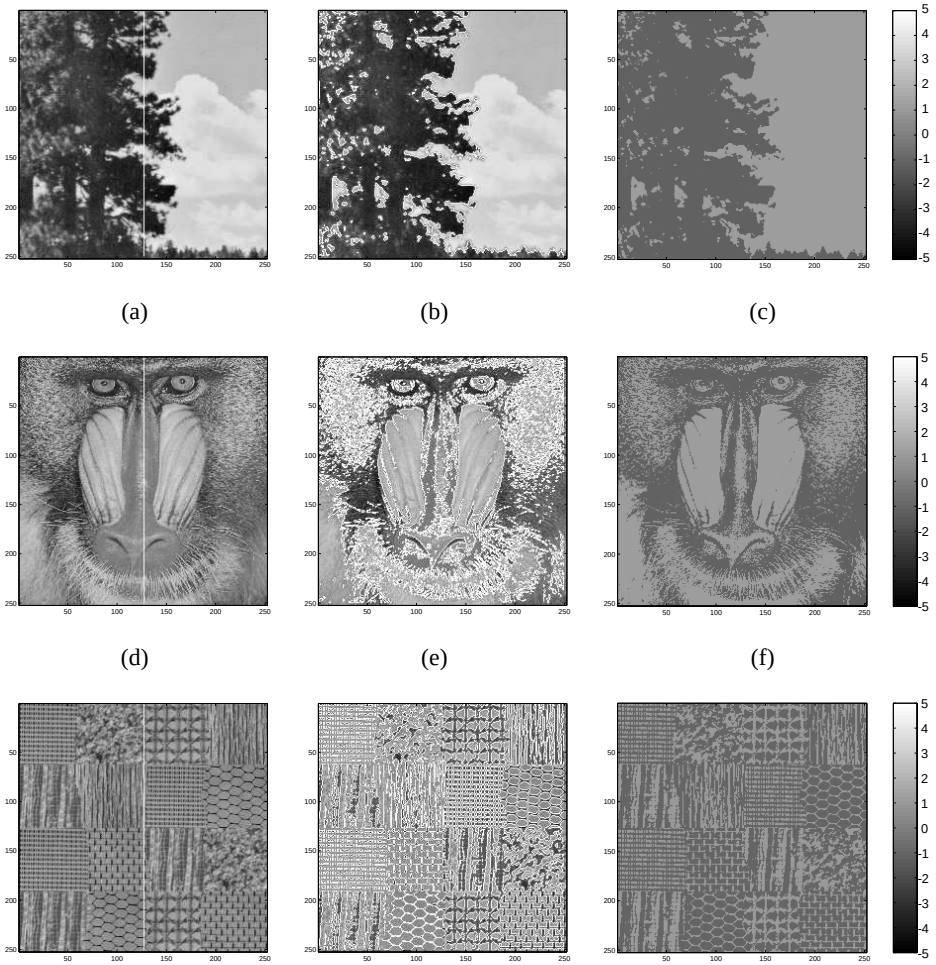

(a) (b) (c)

(d) (e) (f)

(g) (h) (i)

Fig. 6. Segmentation results on real images. For all images, $\alpha = 1$. First column: initial zero level set with the proposed initialization. Second column: final segmentation result. Third column: shows the ϕ function of the final segmentation result.

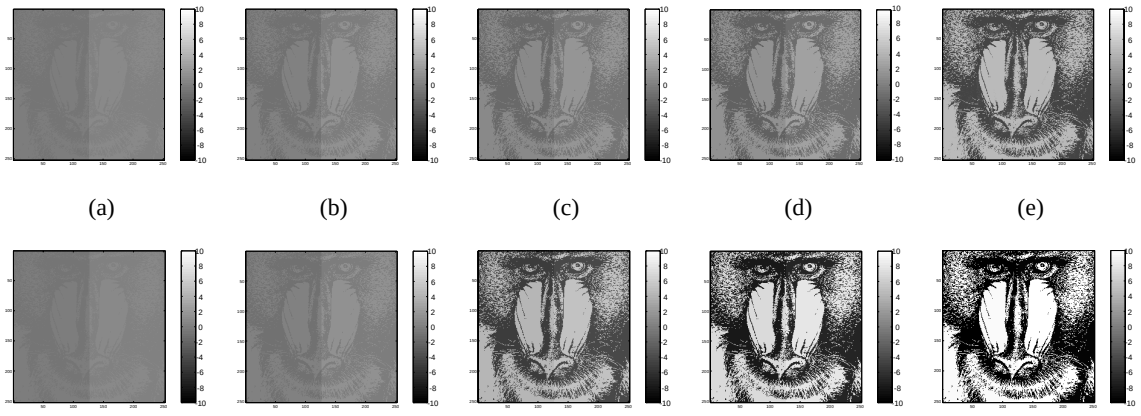

(a) (b) (c) (d) (e)

(f) (g) (h) (i) (j)

Fig. 7. Effect of the α parameter. Top row: showing the evolution of the ϕ function with $\alpha = 4$, after (a) 1 iteration (b) 3 iterations (c) 4 iterations (d) 6 iterations (e) 8 iterations. Bottom row: showing the evolution of the ϕ function with $\alpha = 10$, after (f) 1 iteration (g) 4 iterations (h) 9 iterations (i) 14 iterations (j) 18 iterations.

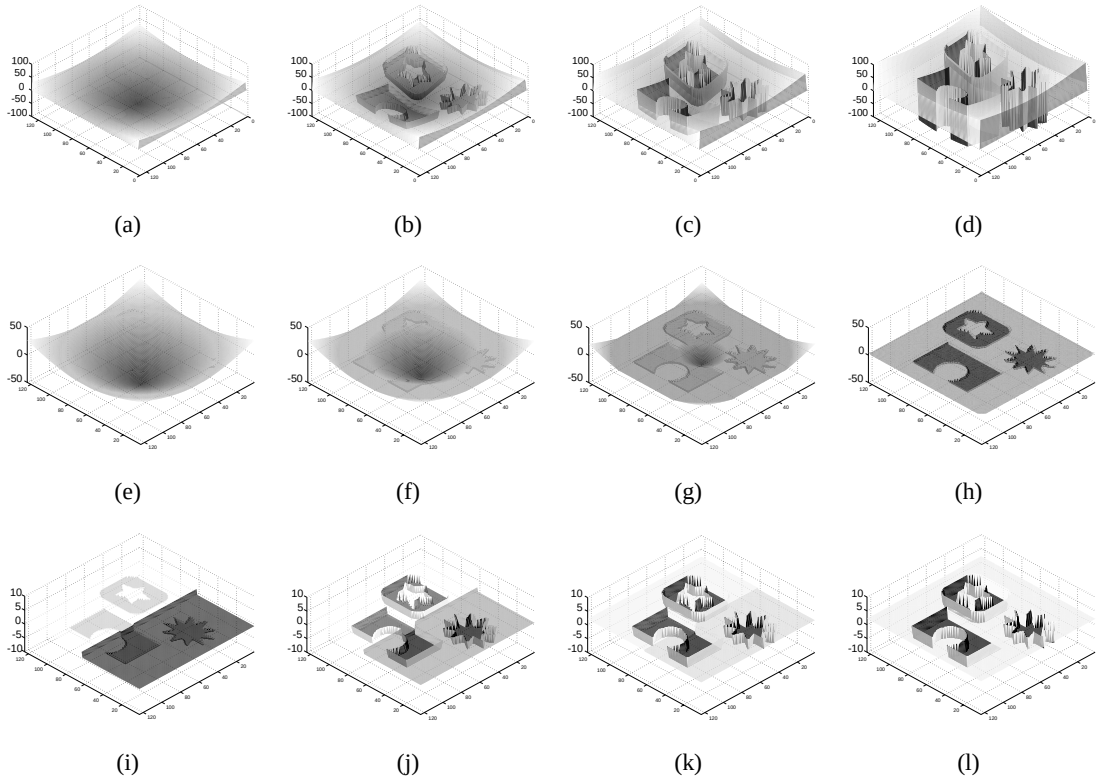

(a) (b) (c) (d)

(e) (f) (g) (h)

(i) (j) (k) (l)

Fig. 8. Showing the evolution of the ϕ function of the Chan-Vese model and the proposed model. For the proposed model, $\alpha = 1$. Top row: evolution of ϕ function with the regularized Chan-Vese model. Here, (d) is not the convergence state, and the magnitude of ϕ keeps growing. Middle row: evolution of ϕ function with the proposed model, initialized with a signed distance function. Here, (h) is the convergence state. Bottom row: evolution of ϕ function with the proposed model, with proposed initialization . Here, (l) is the convergence state.

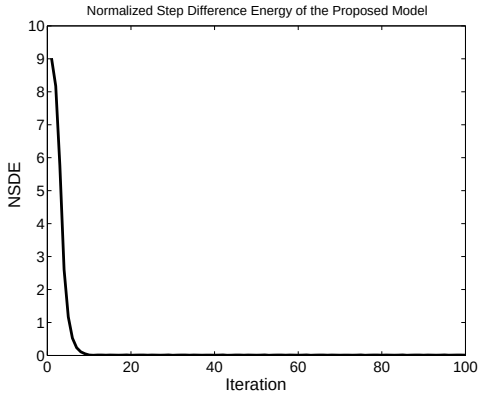

Fig. 9. The normalized step difference energy of the proposed model.